Molecules and Cells

Negative Regulation of Erythroid Differentiation via the CBX8-TRIM28 Axis

Hyun Jeong Kim, Jin Woo Park, Joo-Young Kang, and Sang-Beom Seo*

Department of Life Science, College of Natural Sciences, Chung-Ang University, Seoul 06974, Korea
*Correspondence: sangbs@cau.ac.kr
https://doi.org/10.14348/molcells.2021.0012
www.molcells.org

Although the mechanism of chronic myeloid leukemia (CML) initiation through BCR/ABL oncogene has been well characterized, CML cell differentiation into erythroid lineage cells remains poorly understood. Using CRISPR-Cas9 screening, we identify Chromobox 8 (CBX8) as a negative regulator of K562 cell differentiation into erythrocytes. CBX8 is degraded via proteasomal pathway during K562 cell differentiation, which activates the expression of erythroid differentiation-related genes that are repressed by CBX8 in the complex of PRC1. During the differentiation process, the serine/threonine-protein kinase PIM1 phosphorylates serine 196 on CBX8, which contributes to CBX8 reduction. When CD235A expression levels are analyzed, the result reveals that the knockdown of PIM1 inhibits K562 cell differentiation. We also identify TRIM28 as another interaction partner of CBX8 by proteomic analysis. Intriguingly, TRIM28 maintains protein stability of CBX8 and TRIM28 loss significantly induces proteasomal degradation of CBX8, resulting in an acceleration of erythroid differentiation. Here, we demonstrate the involvement of the CBX8-TRIM28 axis during CML cell differentiation, suggesting that CBX8 and TRIM28 are promising novel targets for CML research.

Keywords: chromobox8, chronic myeloid leukemia, erythroid differentiation, serine/threonine-protein kinase pim-1, tripartite motif containing 28

INTRODUCTION

Hematopoiesis is one type of multi-step processes in our body that can be traced down to hematopoietic stem cell (HSC) self-renewal and stepwise HSC/progenitor cell differentiation (Jagannathan-Bogdan and Zon, 2013). Chronic myeloid leukemia (CML) is developed via clonal myeloproliferative pluripotent HSC malignancy, characterized by the expression of the BCR/ABL1 fusion oncogene located within the Philadelphia chromosome (Zhang and Ren, 1998). K562, one of the human CML cell lines, behaves like undifferentiated early pluripotent hematopoietic progenitors and is widely used as a model for understanding hematological cell differentiation based on its ability to differentiate to either erythroid or megakaryocytic lineage (Tsiftsoglou et al., 2009). Although the cause of CML has been well studied (Deininger et al., 2000), the aspect of differentiation of CML cells has not been precisely elucidated yet.

The CRISPR-Cas9 genome editing system has been recognized as a powerful and effective tool for high-throughput loss of function screening assays (Shalem et al., 2014; Wang et al., 2014). There are lots of studies identifying specific factors as novel therapeutic targets or key regulators of some diseases by using CRISPR screening in various *in vitro/in vivo* systems (Bajaj et al., 2020; Wei et al., 2020). Therefore, in this paper, we utilized this screening technology to find new factors regulating the CML cell differentiation.

CBX8, also known as Pc class 3 homolog (PC3), is a typical subunit of the Polycomb repressive complex 1 (PRC1). The

Received 15 January, 2021; revised 25 April, 2021; accepted 29 April, 2021; published online 13 July, 2021

eISSN: 0219-1032

PRC1 complex is comprised of various Polycomb group proteins (PcG) such as PCGF, CBX and RING1 paralogs and is recruited to H3K27me3 sites through chromodomain of CBX, thereby stabilizing the repression of nearby genes through RING1-mediated H2AK119ub (Wang et al., 2004). Recent studies have demonstrated that various PcG proteins have an effect on both self-renewal of HSCs and differentiation into blood cell types such as erythrocytes, megakaryocytes, and monocytes (Di Carlo et al., 2019). Among them, CBX8 has been reported to be involved in brain development and embryonic stem cell differentiation by regulating gene expression of key factors in the processes (Klauke et al., 2013; Oza et al., 2016). However, the effects and underlying mechanisms of CBX8 during CML cell differentiation are rarely investigated.

As a member of PIM family, PIM1 has a function of serine/threonine kinase (van Lohuizen et al., 1989). It has been reported that, depending on its kinase activity, PIM1 can regulate cell proliferation via inducing phosphorylation-mediated degradation of p21 and myoblast differentiation (Banerjee et al., 2014; Liu et al., 2019). Furthermore, PIM1-deficiency in mouse resulted in the reduction of both body size and hematopoietic cell proliferation (Mikkers et al., 2004). Although there are results showing that PIM1 acts on CBX8 for phosphorylation and reduces protein stability (Zhan et al., 2018), detailed understanding of the relationship between the two factors still remains unclear.

In this study, with the purpose of elucidating the molecular mechanisms of erythroid differentiation in K562 cells, we identified CBX8 as a negative regulator in this process by CRISPR-Cas9 screening. PIM1 is one of the regulators responsible for CBX8 regulation via phosphorylating of serine 196 on the CBX8. Finally, we also showed that the tripartite motif containing 28 (TRIM28) is a novel interacting partner of CBX8 that protects CBX8 from ubiquitination, thereby affecting K562 cell differentiation.

MATERIALS AND METHODS

Plasmid constructs

The pTRIPZ(M)-HT-Cbx8 plasmid was purchased from Addgene (#82516). GST-CBX8 fusion proteins and mammalian expression vectors were constructed by inserting CBX8 into the pGEX-4T1 bacterial expression vector and modified plenti-puro-3Xflag vector (#39481; Addgene). Sequences encoding CBX8 #1 (amino acids 1-130), CBX8 #2 (amino acids 130-305), and CBX8 #3 (amino acids 305-389) were subcloned into the pGEX-4T1 vectors. The PIM1 clone was purchased from Korea Human Gene Bank (hMU012721). PIM1 was also inserted into the pGEX-4T1 bacterial expression vector, as well as the pEGFP-C1 and plenti-puro vector. Double-stranded oligonucleotides for shRNA and sgRNA plasmid construction were produced using primers from the 5' to the 3' end (Supplementary Table S1). These oligonucleotides were then inserted into the *AgeI*/*Eco*RI site of the pLKO.1 TRC vector.

Antibodies

Our study employed antibodies against FK2 (BML-pw-8810-0100, dilution [1:1,000]; Enzo Life Sciences, USA), Phospho-Ser (#9631, dilution [1:5,000]; Cell Signaling Technology, USA), Flag (F3165, dilution into 1 ng/ml; Sigma, USA), APC-CD235A (17-9987-42; eBioscience, USA), CBX8 (sc-374332, dilution [1:2,000]), TRIM28 (sc-515790), PIM1 (sc-13513, dilution [1:1,000]), GFP (sc-9996, dilution [1:2,000]), β-actin (sc-47778 dilution [1:1,000]), H3 (sc-8654, dilution [1:1,000]), and α-tubulin (sc-9103, dilution [1:1,000]) (all from Santa Cruz Biotechnology, USA).

Cell culture

293T was grown in Dulbecco's modified Eagle's medium (DMEM) and K562 in RPMI 1640, each containing 10% heat-inactivated fetal bovine serum and 1% penicillin-streptomycin, at 37°C in a 5% CO_2 atmosphere. 293T cells were transfected with the corresponding DNA constructs using polyethyleneimine (PEI). For differentiation, K562 cells were treated with 30 μM hemin (Sigma). After incubation for 48 h, the cells were harvested and used in downstream experiments. For sodium butyrate-treated cells were treated in 2 mM sodium butyrate for 2 days.

CRISPR-Cas9 screening

CRISPR-Cas9 screening was performed as described in the literature (Doench et al., 2016). Figure 1A illustrates a schematic of the genome-wide CRISPR screening experimental design. Human Brunello pooled library plasmids (total sgRNA 76,441 and 4 sgRNA per a gene) and CRISPR-V2 plasmids (containing Cas9) were obtained from Addgene (#73178 and #52961, respectively) and amplified according to the recommended protocols by electroporation. To produce a lentivirus, 293T cells were transfected in tissue culture dishes at a density of 2×10^6 cells per 100 mm surface area. Plasmid DNA was diluted into medium with a lentiviral packaging plasmid mixture of pMD2.G and pPAX2 and transfected using PEI (3 μg PEI:1 μg DNA). Viral supernatants were collected between 36 h and 72 h after transfection. A lentiviral titer was conducted by transducing the cell line of interest plated at clonogenic density with serial virus dilutions in the presence of 1 μg/ml puromycin. CRISPR-Cas9 screening was performed with a 2-vector system. K562 cells were first infected with lenti-CRISPR-V2 virus and selected using 1 μg/ml puromycin to produce Cas9-expressing K562 cells. These Cas9-expressing K562 cells were then infected with the Brunello pooled library virus (at a multiplicity of infection of 0.3) using polybrene at a density equivalent to 2.5×10^7 cells (~300 cells per a sgRNA) per 150 mm plate area. After 3 days, the K562 cells were cultured and treated with either NaOH (control treatment) or hemin for 3 days. For differentiated cell sorting, hemin-treated cells were washed with phosphate-buffered saline (PBS), resuspended in 1× binding buffer, and stained with CD235A-APC antibodies for 30 min at room temperature in the dark.

CD235A-positive cells were separated with a FACS Aria III system (BD Biosciences, USA) coupled with positive APC staining (total CD235A+ cells). The purity of the sorted fractions exceeded 50% according to fluorescence-activated cell sorting (FACS) analysis.

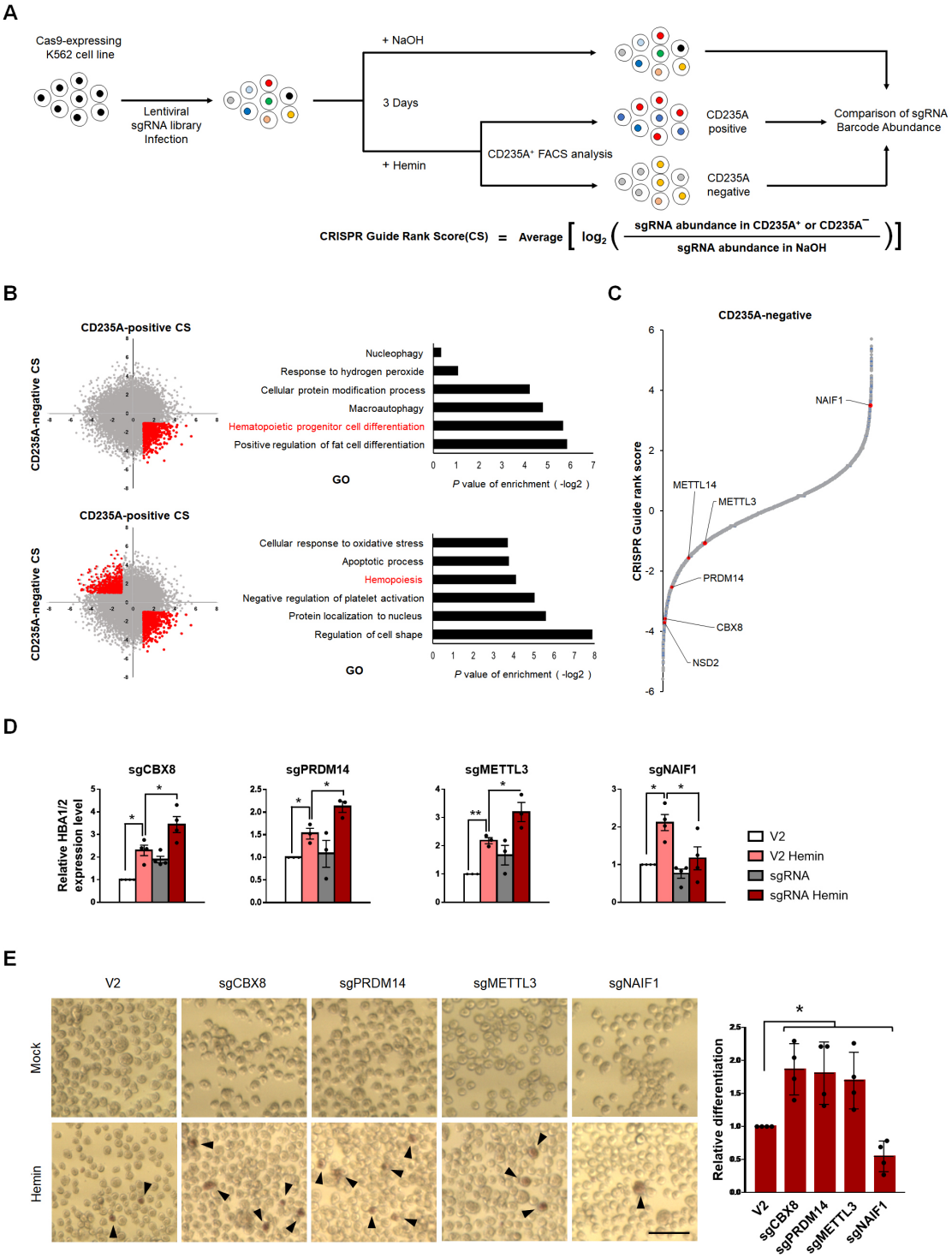

Fig. 1. Genome-wide CRISPR screening reveals CBX8 as a regulator of K562 cell differentiation. (A) Schematic representation of genome-wide CRISPR-Cas9 screening in K562 cells with and without 3 days 30 μM hemin treatment to induce erythroid differentiation. (B) (left) Scatterplots of CS of CD235A-positive versus CD235A-negative K562 cells. (right) Gene ontology analysis of genes in the indicated regions (red). (C) CS (derived from the average of the four sgRNAs CRISPR-Cas9 guide scores within the sgRNAs targeting a given gene) for CD235A-negative K562 cells by hemin sorted after 3 days. Candidate genes and previously identified genes are indicated in red. (D) RT-qPCR of *HBA1/2* in K562 cells with sgV2 (control vector) or sgCBX8, sgPRDM14, sgMETTL3, sgNAIF1 under hemin treatment. (E) (left) Cell differentiation was measured by hemoglobin staining of K562 cells with O-dianisidine. Hemin treatments were conducted for 3 days. Black arrowheads indicate O-dianisidine-positive cells. Scale bar = 25 μm. (right) Quantifications are shown. (D) Values are presented as mean ± SEM (n = 3-4). (E) Values are presented as mean ± SD (n = 4). $*P < 0.05$, $**P < 0.01$; Student's *t*-test.

Next-generation sequencing (NGS) library preparation and sequencing

The sequencing library was prepared by polymerase chain reaction (PCR) amplification methods. Genomic DNA (gDNA) was isolated using the wizard genomic DNA purification kit (Promega, USA) according to the manufacturer's instructions. For NGS library sequencing, 10 parallel PCRs were performed for each given sample. gDNA PCRs were conducted to attach sequencing adaptors and barcode samples, which were divided into multiple 50 μl reactions (total volume) containing a maximum of 5 μg gDNA, P5 stagger primer mix (1 μM), a uniquely barcoded P7 primer (1 μM), and 5X HiPI PCR master mix (Elpis-Biotech). The PCR cycling conditions were the following: an initial 1 min at 95°C; followed by 30 s at 94°C, 30 s at 52.5°C, 30 s at 72°C, for 28 cycles; and a final 10 min extension at 72°C. P5/P7 primers (Supplementary Table S1) were synthesized by Integrated DNA Technologies (IDT, USA). The samples were purified with Agencourt AMPure XP SPRI beads according to the manufacturer's instructions (A63880; Beckman Coulter, USA). The final purified products were then quantified using DNA Picogreen according to the DNA Picogreen Quantification Protocol Guide (QuantiFluor dsDNA system kits for Promega) and qualified using the TapeStation DNA screentape HSD1000 system (Agilent, USA). Afterward, the samples were sequenced in an Illumina HiSeq™ 2500 sequencer (USA). Reads were counted by first searching for the CACCG sequence in the primary read file that appears in the 5′ vector of all sgRNA inserts. The next 20 nts represented the sgRNA insert, which was then mapped to a reference file of all possible sgRNAs present in the library. The reads were then assigned to a condition (e.g., a well on the PCR plate) based on the 8-nt barcode included in the P7 primer. The resulting read count matrix was first normalized to reads per million within each condition with the following formula: reads per sgRNA/total reads per condition $\times 10^6$. The reads per million were then $\log_2$-transformed by first adding 1 to all values, which is necessary to obtain the log of sgRNAs with zero reads.

Data processing and analysis

sgRNA spacer sequences were mapped to the reference human Brunello library. Normalized read counts were obtained by normalizing to total read count per sample. We first selected genes for which three out of four sgRNAs showed common incremental or decremental patterns compared with CD235A-positive cells. CRISPR guide scores were calculated by averaging the log fold change of the normalized sgRNAs lead counts between NaOH or hemin-treated CD235A-positive samples. Gene enrichment and functional annotation analysis for the significant probe list were performed using the DAVID software (http://david.abcc.ncifcrf.gov/home.jsp).

Immunoprecipitation and ubiquitination assays

The 293T cells that were transiently transfected with both flag-CBX8 and GFP-PIM1 were lysed in NP-40 buffer (50 mM Tris-HCl [pH 7.5], 200 mM NaCl, 0.5% NP-40, 1× protease inhibitor cocktail) and the lysates were immunoprecipitated using anti-flag or GFP. Protein A/G agarose beads (GenDEPOT) were then added, and the mixture was gently rotated for 2 h at 4°C. The bound proteins were analyzed by immunoblotting with the appropriate antibodies. The K562 cells used in the IP assay were treated with 30 μM hemin for 48 h. For ubiquitination assays, K562 cells were treated with 20 μM MG132 for 8 h immediately prior to lysis. The cells were then lysed in modified RIPA buffer (50 mM Tris-HCl [pH 7.5], 150 mM NaCl, 0.1% SDS, 0.5% sodium deoxycholate, 1% NP-40, 1× protease inhibitor cocktail, 1 mM PMSF, 5 mM EDTA and 25 mM N-ethylmaleimide [NEM]). The resulting cell lysates were immunoprecipitated using anti-CBX8. Protein A/G agarose beads were then added and the mixture was gently rotated for 2 h at 4°C. Bound proteins were analyzed by immunoblotting with the indicated antibodies.

Reverse transcription and real-time PCR

Total RNA was isolated from viral infected K562 cells using the RNAiso Plus RNA extraction reagent (TaKaRa, Japan). After cDNA synthesis, the cDNA was quantified and used for mRNA expression analysis. The PCR primers are summarized in Supplementary Table S1. Dissociation curves were examined after each PCR run to verify the amplification of a single product of the appropriate length. The mean threshold cycle (C_T) and standard error values were calculated from individual C_T values obtained from triplicate reactions per stage. The normalized mean C_T value was estimated as ΔC_T by subtracting the mean C_T of GAPDH. $\Delta\Delta C_T$ values were calculated as the difference between the control ΔC_T and the values obtained for each sample. The *n*-fold changes in gene expression relative to an untreated control were calculated as $2^{-\Delta\Delta CT}$.

GST-pulldown assay

Cell lysates ectopically expressing pEGFP-PIM1 or pCMV-3X-flag-TRIM28 in 293T cells were incubated with GST-CBX8 wild type (WT) (amino acids 1-389) and GST-CBX8 deletion mutants (amino acids #1, 1-130; #2, 130-305; #3, 305-389) obtained from *Escherichia coli* in TNT reaction buffer (50 mM Tris-HCl [pH 7.6], 150 mM NaCl, 0.1% Triton X-100). Next, the protein complexes were washed three times with TNT washing buffer (50 mM Tris-HCl [pH 7.6], 300 mM NaCl, 0.5% Triton X-100). The precipitated proteins were then separated using 12% SDS-PAGE and then analyzed via western blotting with the appropriate antibodies.

In vitro kinase assay

In vitro kinase assays were performed at 30°C for 3 h in kinase reaction buffer (50 mM Tris-HCl [pH 7.5], 10 mM $MgCl_2$, 0.1 mM EDTA, 2 mM dithiothreitol [DTT] and 10 mCi [^{32}p] ATP [PerkinElmer]). GST-CBX8 WT (amino acids 1-389) and GST-CBX8 deletion mutants (amino acids #1, 1-130; #2, 130-305; #3, 305-389) were incubated with GST-PIM1. The reaction mixtures were separated using 12% SDS-PAGE and analyzed via autoradiography.

LC-MS/MS for phosphorylated peptides analysis

Purified GST-CBX8 was used as a substrate for *in vitro* kinase assays with GST-PIM1. The method was the same as described for the *in vitro* kinase assay section, but replacing the 10 mCi [^{32}p] ATP with non-radioactive 100 μM ATP (AMRES-

CO). After the reaction, the proteins were separated by SDS-PAGE and gel slices from the GST-CBX8 WT and construct #2 were isolated. Nano LC-MS/MS analysis was performed with a nano HPLC system (Agilent). The nano chip column (150 mm × 0.075 mm; Agilent) was used for peptide separation. The mobile phase A for LC separation was 0.1% formic acid in deionized water and the mobile phase B was 0.1% formic acid in acetonitrile. The chromatography gradient was designed for a linear increase from 3% B to 45% B in 30 min, 45% B to 95% B in 1 min, 95% B in 4 min, and 3% B in 10 min. The flow rate was maintained at 300 nl/min. Product ion spectra were collected in information-dependent acquisition (IDA) mode, then analyzed with an Agilent 6530 Accurate-Mass Q-TOF using continuous cycles of one full scan TOF MS from 300-2,000 m/z (1.0 s) plus three product ion scans from 150-2,000 m/z (1.5 s each). Precursor m/z values were selected starting with the most intense ion, using a selection quadrupole resolution of 3 Da. The rolling collision energy feature was used, which determines collision energy based on the precursor value and charge state. The dynamic exclusion time for precursor ion m/z values was 60 s.

Database searching

The mascot algorithm (Matrixscience, USA) was used to identify peptide sequences present in a protein sequence database. Database search criteria were, sequence database; CBX8, fixed modification; carbamidomethylated at cysteine residues; variable modification; oxidized at methionine residues, phosphorylation at serine residues, maximum allowed missed cleavage; 2, MS tolerance; 100 ppm, MS/MS tolerance; 0.1 Da. Only peptides resulting from trypsin digests were considered. The peptides were filtered with a significance threshold of $P < 0.05$.

Subcellular fractionation

Preparation of nuclear and cytosolic fractions was carried out by lysing cells for 10 min on ice using buffer A (10 mM HEPES [pH 7.9], 10 mM KCl, 0.1 mM EDTA, 1 mM DTT, 0.5 mM PMSF, 1× protease inhibitor cocktail, and 0.4% NP-40), followed by centrifugation at 15,000*g* for 3 min. Supernatants were retained as cytosolic fractions, whereas the pellets were subjected to further lysis in buffer B (20 mM HEPES [pH 7.9], 0.4 M NaCl, 1 mM EDTA, 10% glycerol, 1 mM DTT, 0.5 mM PMSF, and 1× protease inhibitor cocktail). The pelleted material was then resuspended by pipetting. After a 2 h agitation at 4°C, lysates were centrifuged at 15,000*g*, and the resulting supernatants were collected as nuclear fractions.

FACS analysis

To measure the K562 differentiation ratio, K562 cells infected with shNC, shPIM1, shTRIM28, and flag-tagged CBX8 and its control vector were treated with 30 μM hemin for three days. The cells were then washed with PBS and resuspend in 1× binding buffer (1% BSA, 1 mM EDTA in PBS), after which anti-APC-CD235A was added for 30 min at 4°C in the dark. Finally, the cells were subjected to FACS analysis using a FACSCalibur system.

Chromatin immunoprecipitation analysis

ChIP analysis was performed as described in the literature (Kim et al., 2008). Briefly, K562 cells were treated with 30 μM hemin for 48 h. The cells were cross-linked by addition of 1% formaldehyde to the medium and incubation for 10 min at 37°C, followed by addition of 125 mM glycine and incubation for 5 min at room temperature. The cells were then lysed in SDS lysis buffer, after which the samples were sonicated and immunoprecipitated using the indicated antibodies. The immunoprecipitates were eluted and reverse cross-linked. The DNA fragments were then purified and PCR amplified for quantification using each PCR primer pair (Supplementary Table S1). Disassociation curves were generated after each PCR run to ensure amplification of a single product of the appropriate length. The mean threshold cycle (C_T) and standard error values were calculated from individual C_T values obtained from duplicate reactions per stage. The normalized mean C_T value was estimated as ΔC_T by subtracting the mean C_T of the input from that of each gene.

O-dianisidine staining

Hemoglobin activity was determined in K562 cells by performing o-dianisidine staining as previously described (Sawafuji et al., 2003). Briefly, K562 cells were cultured with 30 μM hemin for 2 days. To detected hemoglobin synthesis, K562 cells were washed with PBS and stained for 15 min in the dark in 0.6 mg/ml 3,3'-dimethoxy benzidine (Sigma), 0.01 M sodium acetate (pH 4.5), 0.65% H_2O_2 and 40% (v/v) ethanol. The cells were then washed once with PBS and suspended with 70% glycerol in glass slides for microscopy. The percentages of dianisidine-positive cells were calculated by counting four independent fields to obtain the average.

Myeloma tissue array

Formalin-fixed, paraffin-embedded tissue array slides containing bone marrow (BM) tissue (T291d) were purchased from US Biomax (USA). Briefly, after deparaffinization in xylene and rehydration in graded ethanol, endogenous peroxidase activity was blocked by incubating with 3% hydrogen peroxide for 10 min. Next, tissue sections were heated in 100 mM citrate buffer (pH 6.0) for 10 min to retrieve antigens and then preincubated with normal goat serum for 30 min at room temperature. Antibodies against CBX8 (diluted 1:100), H2AK119Ub (diluted 1:200), and TRIM28 (diluted 1:100) were used as the primary antibodies. The specimens were subsequently incubated with biotinylated anti-rabbit or anti-mouse secondary antibodies (Vectastain Laboratories, USA) and streptavidin–horseradish peroxidase (Zymed Laboratories, USA). DAB (3,3-diaminobenzidine; Vectastain Laboratories) was used as a chromogen and eosin was used for counterstaining.

Statistics and reproducibility

All data were reported as the mean ± SEM of three or more independent experiments and ± SD of three technical triplicates from a representative ChIP assay. Statistical significance ($P < 0.05$) was calculated using Microsoft Excel 2016 (Microsoft, USA). Differences between groups were evaluated by one-way ANOVA followed by a Student's *t*-test or Bonferroni

test, as appropriate. Data distributions were clearly illustrated using bar graphs and box plots with standard deviation whiskers.

RESULTS AND DISCUSSION

CBX8 identified as a regulator of K562 cell differentiation by genome-wide CRISPR screening

To identify genes that affect erythroid differentiation of K562 cells, a classic model cell line for CML research, CRISPR-Cas9 screening was conducted using the human Brunello pooled library containing a total of 76,441 sgRNA constructs targeting 19,114 human coding genes (4 sgRNAs per a gene) and the CRISPR-V2 plasmid for Cas9 expression. After three days of hemin treatment to induce erythroid differentiation, the cells were sorted into two groups based on their surface maker expression of CD235A (Ma et al., 2013) (Supplementary Fig. S1A). As a surrogate for differentiation level, CRISPR guide rank score (CS) was analyzed by the enrichment or depletion of sgRNA abundance in the $CD235A^+$ or $CD235A^-$ groups compared with that of the NaOH-treated control group (Fig. 1A). We expected that sgRNAs targeting genes with negative effects on erythroid differentiation would be more depleted in the $CD235A^-$ group but more enriched in the $CD235A^+$ group compared with the control group. Upon performing pathway and gene ontology analyses of sgRNAs that were enriched in $CD235A^+$ group but not in $CD235A^-$ group (Fig. 1B, top; see the fourth quadrant), it was confirmed that these genes are important for hematopoietic differentiation. In addition, we found that several sgRNAs showed the opposite CS distributions in $CD235A^+$ and $CD235A^-$ groups (Supplementary Table S2). Note that pathway analysis of sgRNAs involving these factors also revealed enrichment of genes associated with hemopoiesis (Fig. 1B, bottom). Our genomic screening assays identified multiple previously known dependencies of hematopoietic differentiation on a variety of genes such as METTL3, METTL14 and NSD2 (Park et al., 2020; Vu et al., 2017; Weng et al., 2018) (Fig. 1C, Supplementary Fig. S1B). Notably, several genes were identified as new regulators of erythroid differentiation, including the transcription factor PRDM14 and the apoptosis inducing factors NAIF1 and CBX8, which had not been previously explored in K562 differentiation. For further validation of the screening data, we depleted CBX8, PRDM14, METTL3, and NAIF1 using sgRNAs to target each gene. Among the four genes, METTL3 and NAIF1 were used as controls based on their CS, exerting negative and positive effects on erythroid differentiation respectively. Therefore, sgMETTL3 tended to differentiate more, whereas sgNAIF1 would be less differentiated than V2. CBX8, PRDM14, and METTL3 depletion led to increases in the erythroid-marker gene *HBA1/2* under hemin-treatment and the results accorded with each of CS distribution. However, the sgNAIF1 cell line, whose CS was on the opposite side with other three genes, showed different expression pattern whereby the transcription of *HBA1/2* was less induced by hemin than V2 (Fig. 1D). Our hemoglobin staining assays also demonstrated that three cell lines (sgCBX8, sgPRDM14, sgMETTL3) were more differentiated toward the erythroid lineage under the hemin-treatment than V2, with the sgNAIF1 cell line being the only exception (Fig. 1E). Among these genes, CBX8 emerged as one of the top-ranked genes in the screen and led to the most significant phenotypic changes during K562 cell erythroid differentiation. CBX8, a well-known subunit of the PRC1 complex, has been mostly studied in the field of embryonic development but its role in CML cell differentiation remains poorly understood (Aloia et al., 2013). Therefore, we focused on investigating the mechanisms by which CBX8 regulates erythroid differentiation.

CBX8 is a negative regulator of hemin-mediated K562 cell differentiation

Since we noted the inhibitory role of CBX8 in erythroid differentiation by CRISPR screening, we sought to verify whether the level of CBX8 was altered by hemin. The protein level of CBX8 decreased by exposure to hemin in K562 cells (Fig. 2A). However, the mRNA level was not affected during hemin-mediated differentiation (Fig. 2B). Treatment with the proteasome inhibitor MG132 restored CBX8 protein levels in hemin-treated K562 cells, indicating that the reduction of CBX8 occurs via proteasome-dependent pathway (Fig. 2C). Protein ubiquitination is a key step in the proteasomal degradation pathway (Jiang and Chen, 2011) and we identified that hemin increased CBX8 poly-ubiquitination by an immunoprecipitation (IP)-based ubiquitination assay (Fig. 2D). Upon testing sodium butyrate, another known erythroid differentiation inducer (Sutherland et al., 1986), the same results of decreased CBX8 proteins were observed; however, the transcription of CBX8 was still not affected (Supplementary Figs. S2A and S2B). The reduction of CBX8 was rescued by MG132 (Supplementary Fig. S2C). As expected, CBX8 ubiquitination was also up-regulated during sodium butyrate-mediated differentiation (Supplementary Fig. S2D). After confirming that CBX8 protein levels decreased upon exposure to erythroid differentiation inducers, we sought to investigate whether CBX8 overexpression would have the opposite effect. To test this, flag-tagged CBX8-expressing K562 cells were generated (Fig. 2E). While CBX8 depletion by sgRNA led to increase in *HBA1/2* expression (Fig. 1D), overexpression of CBX8 resulted in relatively smaller increase in hemin-induced *HBA1/2* expression than control cells (Fig. 2F). FACS analysis based on CD235A also revealed that erythroid differentiation occurred more vigorously in control cells than flag-tagged CBX8-expressing cells (Fig. 2G).

Taken together, these results suggest that when K562 cells undergo hemin- or sodium butyrate-induced erythroid differentiation, CBX8 decreases in a proteasome-dependent manner and acts as a negative regulator of the differentiation.

Loss of CBX8 induces transcriptional activation of erythroid differentiation-related genes

The PRC1 complex involving CBX8 promotes transcriptional repression by accumulation of H2AK119ub (Koppens and van Lohuizen, 2016). As shown in Fig. 2, CBX8 decreased in response to hemin and its subcellular localization was predominantly linked to the nuclear fraction (Fig. 3A) (Vandamme et al., 2011). Therefore, we hypothesized that some CBX8 target genes are differentially expressed and involved in CBX8-dependent regulation of erythroid differentiation.

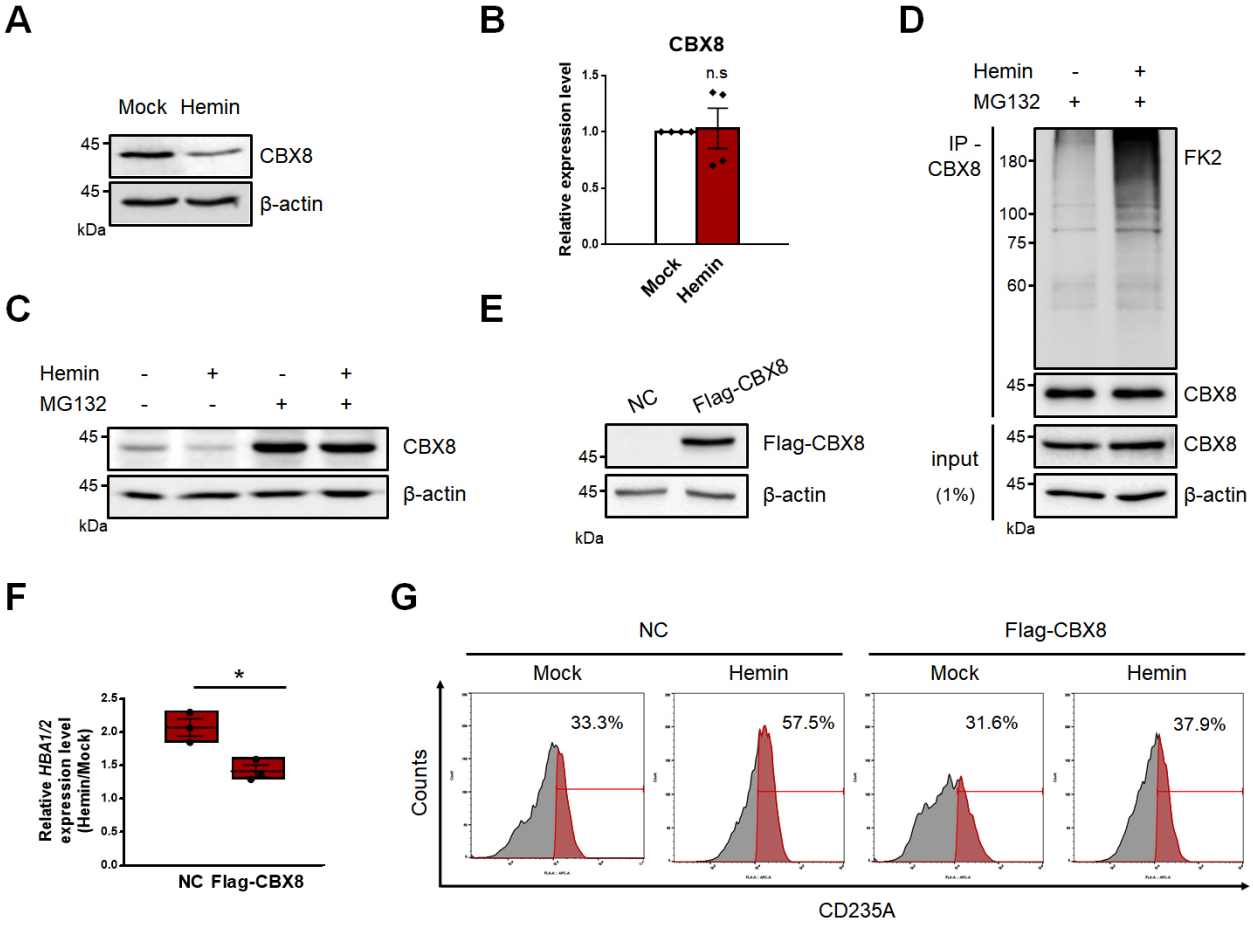

Fig. 2. CBX8 negatively regulates hemin-mediated K562 cell differentiation. (A) Immunoblots were performed using K562 cell lysates, which were treated with 30 μM hemin for 2 days. (B) RT-qPCR of *CBX8* was performed using K562 cells treated with 30 μM hemin for 2 days. n.s, not significant. (C) Immunoblots were performed using K562 cell lysates, which were treated with 30 μM hemin for 2 days and 20 μM MG132 proteasome inhibitor for 8 h before harvested. (D) IP of endogenous CBX8 in K562 cells was performed to investigate polyubiquitination chains of CBX8. Cell lysates were immunoprecipitated using anti-CBX8 antibodies, and polyubiquitination chains were immunoblotted using FK2 antibodies that detect mono- and poly-ubiquitin. (E) Overexpression of flag-tagged CBX8 was confirmed by immunoblots. NC, normal control. (F) RT-qPCR of *HBA1/2* was performed using K562 cells stably expressing flag-tagged CBX8. The relative increase of expression in cells treated with 30 μM hemin for 2 days was quantified compared to that of a mock experiment. (G) Histogram showing erythroid differentiation upon 30 μM hemin treatment for 3 days. K562 cells expressing control vector (NC) or flag-tagged CBX8 were stained with anti-APC-CD235A and FACS sorted. (B and F) Values are presented as mean ± SEM (n = 3-4). $*P < 0.05$; Student's *t*-test.

Chromatin immunoprecipitation-sequencing (ChIP-seq) data was used to identify genomic loci bound by CBX8 and PRC1/2 complexes (Bracken et al., 2006). In order to understand the underlying mechanism of hemin-mediated erythroid differentiation of CBX8-depleted cells, *TAL1*, *HOXC4*, and *OVOL2* expressions were investigated. *TAL1* gene, also known as *SCL* or *TCL5*, has been identified during the differentiation of erythroid, megakaryocytic, and basophilic lineages (Mouthon et al., 1993). Previous research has demonstrated that *TAL1* knockdown suppressed erythroid differentiation in K562 cells (Zhou et al., 2012) and that overexpression of *TAL1* increased the rate of erythroid differentiation (Aplan et al., 1992). *HOXC4* is another crucial gene during erythroid lineage differentiation (Bhatlekar et al., 2018). Similar to the *TAL1* gene, the overexpression of human *HOXC4* resulted in the expansion of early and committed myeloid and erythroid progenitors (Daga et al., 2000). In addition to the two erythroid differentiation-related genes, we also investigated the *OVOL2* gene as a typical Polycomb target gene (Fursova et al., 2019). Before the experiments, the sgRNA-mediated depletions of CBX8 were confirmed by alignment of DNA sequences of clonal knock-out cells of *CBX8* with WT cells and clones of sgCBX8#1 were used (Fig. 3B). CBX8 depletion resulted in about 1.5- to 2.5-fold increase in all three genes (Fig. 3C). Consistent with this, the expression of the three genes increased by approximately 1.2–1.5-fold in response to hemin treatment (Fig. 3D). Therefore, the data suggested that the increased expressions of these target genes might

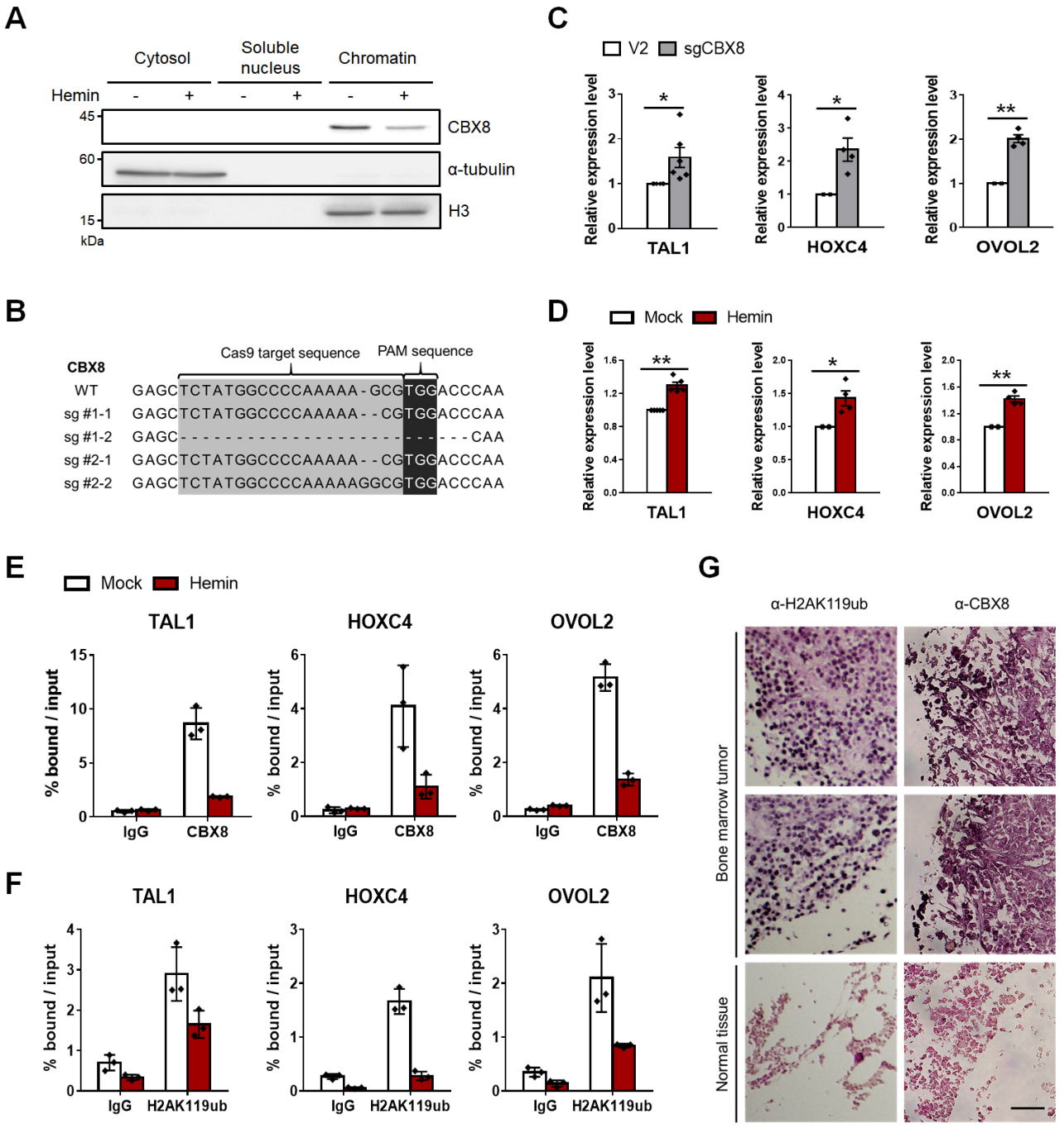

Fig. 3. Loss of CBX8 activates erythroid differentiation-related gene. (A) Fractionation followed by immunoblot showed the localization of CBX8. K562 cells were treated with 30 μM hemin for 2 days and total proteins were separated into cytoplasmic and nuclear fractions. H3 and α-tubulin were used as loading controls for nuclear and cytoplasmic fractions, respectively. (B) Alignment of the nucleic acid sequences of clonal KO cells of *CBX8* with WT cells. sgRNA targeting sites are in gray box. PAM sites are indicated in black box. (C) RT-qPCR results showing the relative expression levels of *TAL1, HOXC4*, and *OVOL2* in sgV2 and sgCBX8 K562 cells. (D) RT-qPCR results showing the relative expression levels of *TAL1, HOXC4,* and *OVOL2* in K562 cells treated with 30 μM hemin for 2 days. (E and F) K562 cells were treated with 30 μM hemin for 2 days. ChIP employing anti-IgG, anti-CBX8, and anti-H2AK119ub antibodies was then performed. The immunoprecipitated DNA fragments from the promoter regions of *TAL1, HOXC4,* and *OVOL2* were analyzed by qPCR. All experiments were performed three times with similar results. (G) Formalin-fixed tissue array slides from BM tissues were used for 3,3-diaminobenzidine (DAB) staining of CBX8 and H2AK119ub for immune-histochemistry assays. Scale bar = 25 μm. (C and D) Values are presented as mean ± SEM (n = 4-5). $*P < 0.05$, $**P < 0.01$; Student's *t*-test. (E and F) Values are presented as mean ± SD of technical triplicates from a representative experiment.

be at least partially involved in the accelerated erythroid differentiation of CBX8-depleted cells. To determine whether these genes were indeed the functional downstream targets of CBX8 and the PRC1 complex, levels of CBX8 and H2AK119ub around the promoters were determined by ChIP-qPCR. The CBX8 around the promoter of the three genes decreased under hemin treatment, coupled with a reduction of H2AK119ub mark (Figs. 3E and 3F). Aberrant erythropoiesis has been linked to hematopoietic malignancy (Whichard et al., 2010). Therefore, our study sought to examine the expressions of CBX8 and H2AK119ub in human BM tissue, which is where hematopoietic stem/progenitor cells are located (Dzierzak and Philipsen, 2013). Immunohistochemistry (IHC) assays of BM tissue further supported the notion that both CBX8 and H2AK119ub marks are enriched in tumors compared to the normal adjacent tissues (Fig. 3G). Taken together, these results revealed that the hemin-induced CBX loss promoted erythroid differentiation in K562 cells via the activation of specific PRC1 target genes involving erythroid-related genes such as *TAL1* and *HOXC4*.

PIM1 phosphorylates CBX8 during hemin-mediated K562 cell differentiation

Previous research has revealed that PIM1 phosphorylates CBX8 and promotes degradation in human diploid fibroblast (Zhan et al., 2018). Therefore, we investigated whether PIM1 would also act as a kinase for CBX8 during K562 cell differentiation. PIM1 is transcriptionally activated in response to hemin in K562 cells (Park et al., 2020) (Fig. 4A). It was followed by up-regulation of PIM1 protein levels (Fig. 4B). Moreover, CBX8 phosphorylation level increased upon hemin exposure, suggesting that the up-regulated PIM1 might have participated in the step of CBX8 phosphorylation during the erythroid differentiation (Fig. 4C). We then performed IP of endogenous CBX8 and observed CBX8 interacted with PIM1 in K562 cells (Supplementary Fig. S3A). In addition, the interaction was further promoted by hemin (Fig. 4D). Although CBX8 is known to possess an N-terminal chromodomain and the C-terminal repressor box, a recent comparative sequence analysis between the various Polycomb homologs has identified other motifs in CBX8 (Hemenway et al., 2001; Oza et al., 2016; Senthilkumar and Mishra, 2009) (Supplementary Fig. S3B). Given that the CBX8 contains various domains, we next sought to determine which of domains mediates the interaction between CBX8 and PIM1 by generating a series of GST-tagged CBX8 deletion constructs (Supplementary Fig. S3B). GST-CBX8 pulldown assays followed by western blotting with GFP antibody showed that both the N-terminal and C-terminal regions of CBX8, including the Chromo, ATHL1, RED, and C-box domains, were required for its interaction with PIM1 (Fig. 4E). Besides the interaction, an *in vitro* kinase assay revealed that CBX8 was indeed phosphorylated by PIM1 and the level of CBX8 phosphorylation was in proportion to the amount of PIM1 (Fig. 4F). To further narrow down domains involving the PIM1-phosphorylated residue, an *in vitro* kinase assay was performed using GST-CBX8 constructs and GST-PIM1. Although CBX8 WT and deletion construct #2 were robustly phosphorylated by PIM1, N-terminal and C-terminal CBX8 region phosphorylation was not detected (Fig. 4G). The precise PIM1 phosphorylation sites on CBX8 have not been mapped, which prompted us to identify the specific residues targeted by PIM1. *In vitro* kinase assays using CBX8 WT and deletion construct #2 with PIM1 coupled with LC-MS/MS analysis revealed that serine 196 on CBX8 might be phosphorylated (Fig. 4H). Intriguingly, the serine 196 residue has been reported to be phosphorylated in humans (Bodenmiller et al., 2008). In addition, knockdown of PIM1 reduced the induction of poly-ubiquitination on CBX8 by hemin (Supplementary Figs. S3C and S3D). Our results suggested that PIM1 phosphorylated CBX8 during hemin-induced erythroid differentiation. PIM1 participated in the reduction of CBX8 and affected the differentiation of K562 cells. When CD235A expression levels were analyzed by FACS, the knockdown of PIM1 inhibited the differentiation of K562 cells (Fig. 4I). Collectively, these data revealed that PIM1 could affect the erythroid differentiation in K562 cells upstream of CBX8.

The TRIM28-CBX8 axis regulates erythroid differentiation

Given that CBX8 was degraded in a proteasome-dependent manner by exposure to hemin, we sought to identify the E3 ligase responsible for CBX8 degradation through IP-mass spectrometry (MS) using K562 cells stably expressing flag-tagged CBX8. Notably, we identified PHC1 and PHC3, two well-known Polycomb group proteins associated with the canonical PRC1 complex (Morey and Helin, 2010). TRIM33, which has been reported to recruit CBX8 to DNA damage sites for repair, was also analyzed in our MS results (Oza et al., 2016) (Fig. 5A). However, although there were several proteins with RING or HECT domains that can mediate ubiquitination or are related to ubiquitination, knockdown of these proteins had no significant effect on CBX8 levels (data not shown). Among the proteins in the MS data, TRIM28 was identified as an interaction partner with CBX8 in hemin-treated condition. To validate the analysis, we performed IP of endogenous CBX8 in K562 cells and observed that TRIM28 interacted with CBX8 and it was enforced by hemin (Fig. 5B). Further, we overexpressed flag-tagged TRIM28 in 293T cells and performed a GST-pulldown assay with GST-CBX8 deletion mutants. These experiments revealed that the N-terminal of CBX8 mediated the interaction with TRIM28 (Fig. 5C). TRIM28 is a member of the TRIM family and, as a RING domain protein, it has been shown to target p53 and AMPK for ubiquitination and degradation through proteasome-dependent pathways (Doyle et al., 2010; Pineda et al., 2015). Even though we expected that TRIM28 would be an E3 ligase for CBX8, CBX8 showed significant decreases in TRIM28 knockdown cells (Fig. 5D). To our surprise, when hemin was added, decreases in CBX8 were accelerated further (note that the level of TRIM28 did not change) (Fig. 5E). In fact, some E3 ligases are known to stabilize proteins, which is the opposite role of their degradation-promoting property. For example, TRIM39 has been shown to stabilize Cactin and MOAP-1 by inhibiting the poly-ubiquitination process (Lee et al., 2009; Suzuki et al., 2016). Moreover, another study suggested that TRIM28 protects TRIM24 from degradation (Fong et al., 2018). Therefore, we sought to explore the mechanism that led to CBX8 decreases in TRIM28 knockdown cells and the role of TRIM28 in K562 cell differentiation. When

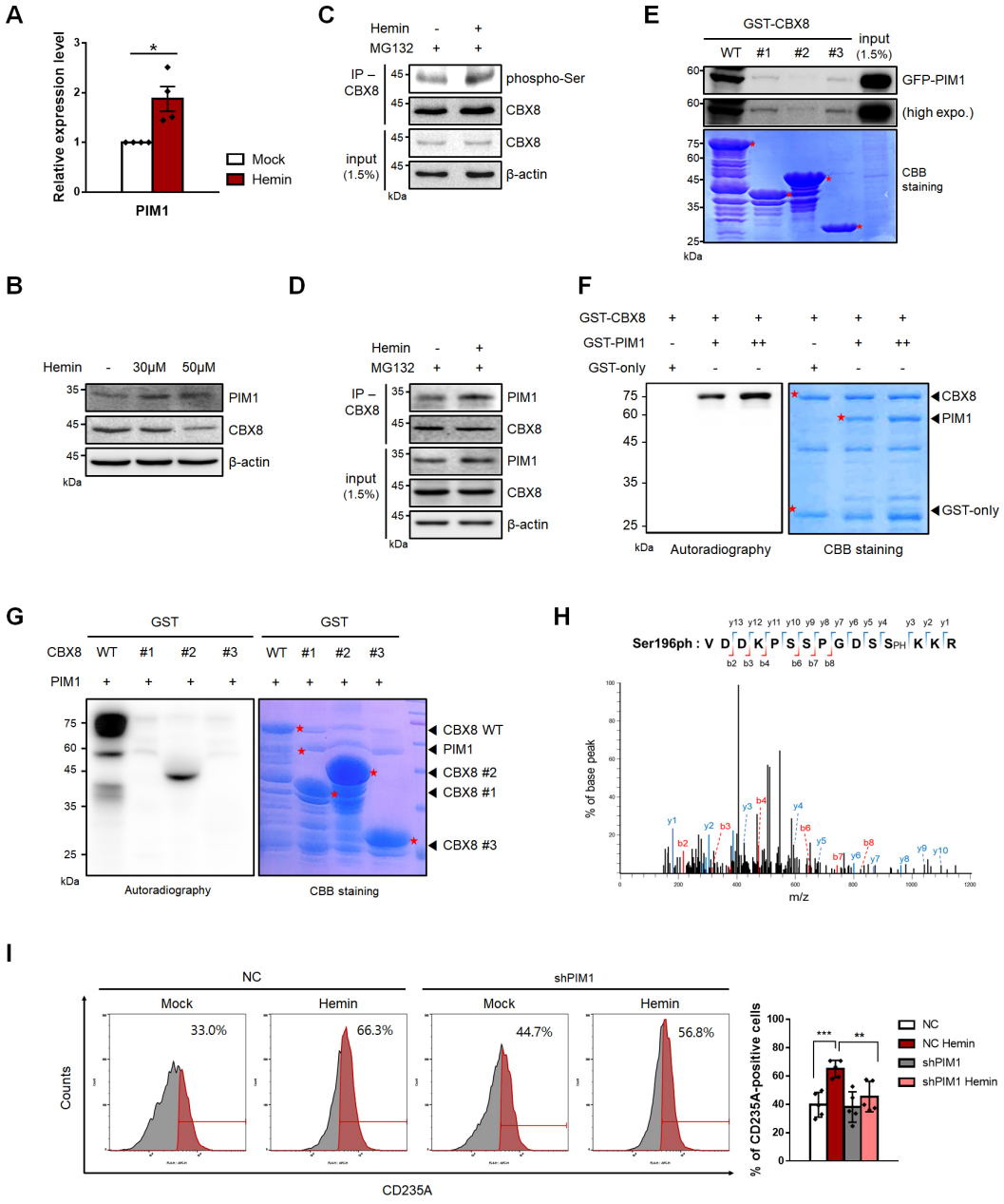

Fig. 4. Phosphorylation of serine 196 on CBX8 by PIM1 affects K562 cell differentiation. (A) RT-qPCR of *PIM1* was performed using K562 cells treated with 30 μM hemin for 2 days. (B) Immunoblots were performed using K562 cell lysates, which were treated with 30 μM, 50 μM hemin for 2 days. (C) IP of endogenous CBX8 in K562 cells was performed and proteins were immunoblotted with the indicated antibodies. (D) IP of endogenous CBX8 was performed using K562 cells treated with 30 μM hemin for 2 days and proteins were immunoblotted with the indicated antibodies. (E) GST-CBX8 WT and deletion constructs were used for GST pulldown assay with 293T cell lysates transiently expressed GFP-tagged PIM1, followed by elution and separation by SDS-PAGE. The amount of GST-CBX8 WT or deletion constructs were determined by Coomassie brilliant blue (CBB) staining. (F) *In vitro* kinase assay using GST-CBX8 and GST-PIM1. The phosphorylated GST-CBX8 by PIM1 were visualized via autoradiography and the amounts of GST-fusion proteins used in the assay are shown in the CBB staining. (G) *In vitro* kinase assay using GST-CBX8 deletion mutants and GST-PIM1. The phosphorylated GST-CBX8 WT and #2 deletion mutant were visualized via autoradiography. The amounts of GST-fusion proteins used in the assay are shown in the CBB staining. (H) GST-CBX8 modified with phosphorylation on serine 196. Mass spectrometry analysis (LC-MS/MS) was performed after *in vitro* kinase assay with GST-CBX8 and GST-PIM1. The graph shown in this panel is based on the data from GST-CBX8 WT. (I) (left) Histogram showing erythroid differentiation induced by 30 μM hemin treatment for 3 days. Stable control and shPIM1 K562 cells were stained with anti-APC-CD235A and sorted by FACS. (right) Quantification of FACS data is shown. NC, normal control. (A) Values are presented as mean ± SEM (n = 4). $*P < 0.05$; Student's *t*-test. (I) Values are presented as mean ± SD (n = 5). $**P < 0.01$, $***P < 0.001$; Student's *t*-test.

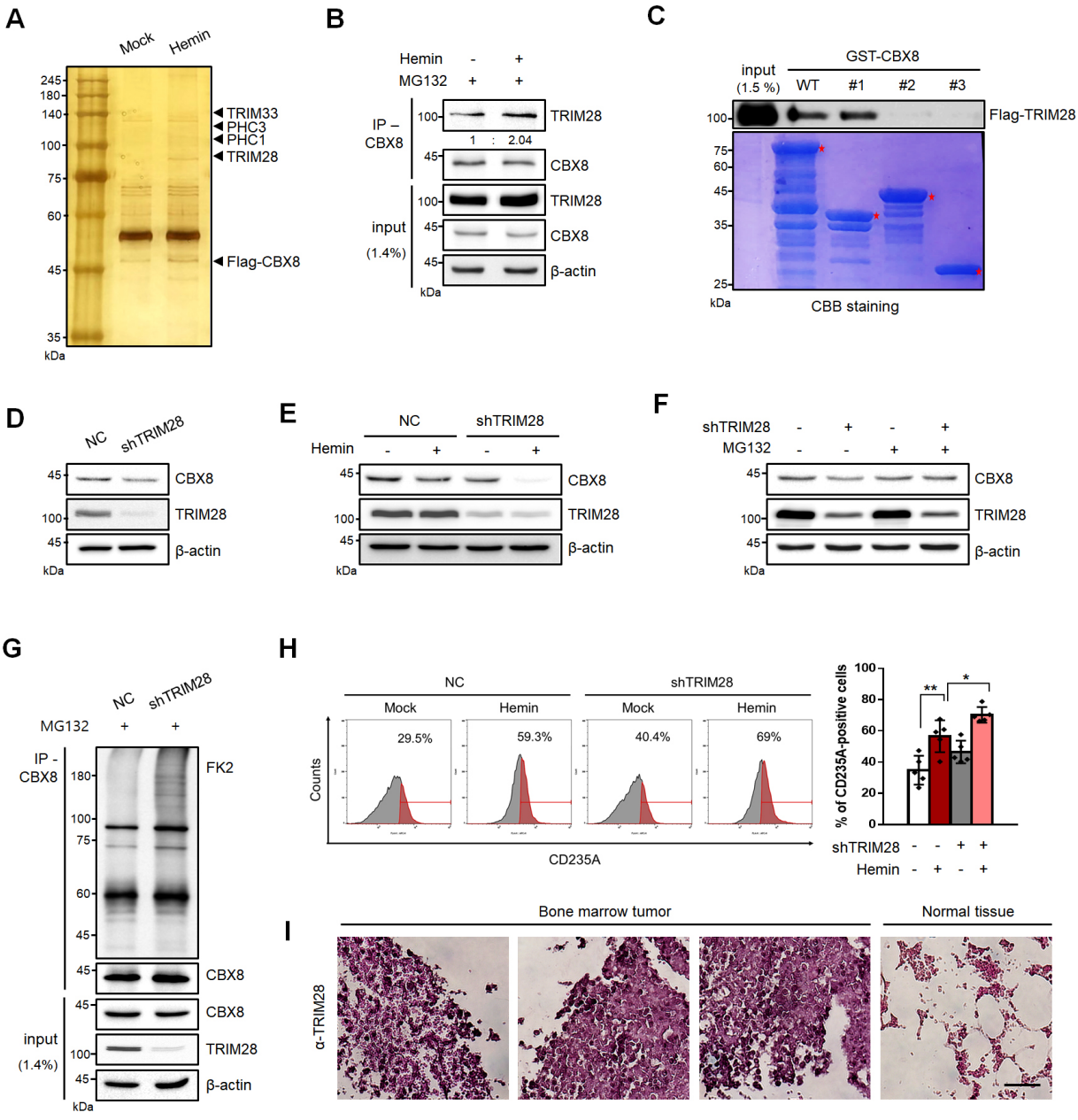

Fig. 5. TRIM28 induces CBX8 protein stabilization. (A) K562 cells stably expressing flag-tagged CBX8 were treated with 30 μM hemin for 2 days. Proteins in complexes with flag-tagged CBX8 were separated by SDS-PAGE after immunoprecipitation and visualized via silver staining. (B) IP of endogenous CBX8 in K562 cells was performed to confirm the interaction between TRIM28 and CBX8. K562 cells were treated with 30 μM hemin for 2 days and MG132 for 8 h before harvested. (C) GST-CBX8 WT and deletion mutants were used for GST pulldown assays. Extracts of 293T cells transiently expressing flag-tagged TRIM28 were incubated with GST-CBX8 or GST-CBX8 deletion mutants followed by elution and separation by SDS-PAGE. The amount of GST-CBX8 WT or deletion constructs were determined by CBB staining. (D) Immunoblots were performed using normal control (NC) and shTRIM28 K562 cells. (E) Immunoblots were performed using NC and shTRIM28 K562 cells treated with 30 μM hemin for 2 days. Each protein was blotted with the indicated antibodies. (F) Immunoblots were performed using NC and shTRIM28 K562 cells, treated with 30 μM hemin for 2 days and 20 μM MG132 for 8 h before being harvested. (G) IP of endogenous CBX8 in K562 cells was performed to investigate polyubiquitination chains of CBX8. NC and shTRIM28 K562 cells were treated with 20 μM MG132 for 8 h before harvested. Cell lysates were immunoprecipitated using anti-CBX8 antibodies and polyubiquitination chains were immunoblotted using FK2 antibodies. (H) (left) Histogram showing erythroid differentiation induced by 30 μM hemin for 3 days. Stable control and shTRIM28 K562 cells were stained with anti-APC-CD235A and sorted by FACS. (right) Quantification of FACS data is shown. Values are presented as mean ± SD (n = 5). $*P < 0.05$, $**P < 0.01$; Student's *t*-test. (I) Formalin-fixed tissue array slides from BM tissues were used for 3,3-diaminobenzidine (DAB) staining of TRIM28 for immuno-histochemistry assays. Scale bar = 25 μm.

treated with MG132, a proteasome inhibitor, the protein level of CBX8 was recovered in shTRIM28 cells, indicating that CBX8 was degraded through a proteasome-dependent pathway in the depletion of TRIM28 (Fig. 5F). These results were further supported by the IP-based ubiquitination assay, which demonstrated an increased polyubiquitination of CBX8 in the TRIM28 knockdown cells (Fig. 5G). To examine the functional role of TRIM28 in erythroid differentiation of K562 cells, we compared the expression level of CD235A through FACS analysis. CD235A-positive cells under hemin-treatment increased when the TRIM28 was depleted compared to the control, suggesting that this increase in differentiated cells was due to CBX8 loss (Fig. 5H). Overall, these results revealed that the interaction between TRIM28 and CBX8 increased during K562 cell differentiation and that TRIM28 might be a protector of CBX8 given that shTRIM28 led to loss of CBX8, thereby promoting erythroid differentiation. In IHC assay, we identified that TRIM28 protein levels were higher in BM malignant tumor tissue compared to that of normal tissue (Fig. 5I). This was further supported by the Gene Expression database of Normal and Tumor tissues 2 (GENT2), showing that TRIM28 mRNA expression level is higher in blood-related cancer patients and cell lines than their normal counterparts (Park et al., 2019) (Supplementary Fig. S4). These results suggest that TRIM28 could be a negative effector in hematopoietic pathogenesis including CML progression.

Here, we revealed that CBX8 inhibits erythroid differentiation of K562 cells by repression of erythroid lineage-related genes (Fig. 6). In K562 cells, CBX8 contributes to the repression of these genes as a part of the PRC1 complex, which is responsible for catalyzing repressive histone mark H2AK119ub. At the same time, the protein level of CBX8 remains quite constant, as TRIM28 prevents CBX8 polyubiquitination. However, when erythroid differentiation is induced, CBX8 degradation occurs via the proteasomal pathway, leading to a decrease in H2AK119ub at the promoter region of the erythroid differentiation-related genes. During this process, two factors are involved in the regulation of CBX8 levels. First, PIM1 is upregulated by hemin and CBX8 becomes more phosphorylated, thereby becoming an enzymatic target of PIM1. Although we couldn't see any change in CBX8 level, knockdown of PIM1 resulted in less differentiated phenotypes according to FACS, indicating that there are other modulators of the CBX8 protein. Second, we identified that TRIM28 has a role in stabilizing CBX8. TRIM28 interacts more strongly when hemin treatment promotes CBX8 degradation, suggesting that it inhibits the rapid decrease of CBX8 or maintains a minimal level of CBX8. Therefore, we speculate that TRIM28 affects the erythroid differentiation of K562 cells during the aforementioned process.

Since abnormal erythropoiesis can lead to various diseases including thrombocytopenia, anemia, and leukemia, uncovering the detailed mechanisms of erythropoiesis could facilitate the identification of novel regulators and new therapeutic strategies to treat blood related malignancies (Beguin, 1999). Although the mechanisms of CML initiation have been widely discussed, little is known about CML differentiation. Chemotherapy with tyrosine kinase inhibitors (TKIs) is the most common treatment strategy for CML; however, these drugs are effective only at the chronic phase, making both accelerated- and blast crisis phase-patients difficult to be cured (Saussele and Silver, 2015). Also, the development of TKIs-resistance remains a major clinical challenge (Bixby and Talpaz, 2009). Therefore, the discovery of novel therapeutic agents and strategies are important to improve the prognosis of CML patients. Moreover, although K562 is undifferentiated and in the pluripotent hematopoietic progenitor niche, it also possesses the ability to differentiate (Tsiftsoglou et al., 2009).

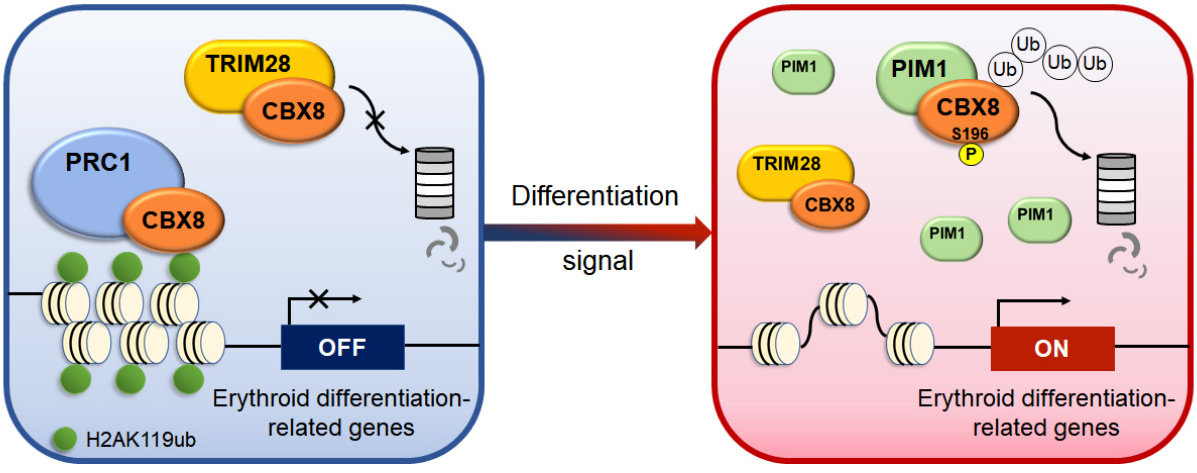

Fig. 6. Graphical model of how CBX8 regulates erythroid differentiation of K562 cells. Schematic representation of the K562 cell differentiation mechanisms. The loss of CBX8 promotes the expression of target genes related to erythroid differentiation by hemin treatment. In an uninduced state, CBX8 in complex of PRC1 represses genes that promote erythroid differentiation. TRIM28 interacts with CBX8 to induce CBX8 protein stability. When erythroid differentiation inducers are added, PIM1 upregulation promotes phosphorylation of CBX8 on serine 196 and induces proteasomal degradation. H2AK119ub levels on promoters of erythroid-related genes decrease via loss of CBX8 and K562 cells undergo erythroid differentiation.

Since stalled differentiation is considered as a characteristic of leukemia, and therefore promoting leukemia cell differentiation has become the focus of medical research (Bruserud et al., 2000; Park et al., 2018). In this respect, our study provides a potential molecular pathway to induce the differentiation of CML cells, suggesting that CBX8 and TRIM28 are promising therapeutic targets for future clinical research.

Note: Supplementary information is available on the Molecules and Cells website (www.molcells.org).

ACKNOWLEDGMENTS

This research was supported by the Chung-Ang University Graduate Research Scholarship in 2019 and by the Basic Science Research program through the National Research Foundation of Korea (NRF-2020R1F1A1064241).

AUTHOR CONTRIBUTIONS

S.B.S. and H.J.K. designed the experiments and analyzed the results. H.J.K., J.W.P., and J.Y.K. performed experiments and analyzed the results. S.B.S. and H.J.K. wrote the manuscript.

CONFLICT OF INTEREST

The authors have no potential conflicts of interest to disclose.

ORCID

Hyun Jeong Kim https://orcid.org/0000-0002-4048-3292
Jin Woo Park https://orcid.org/0000-0002-9382-0598
Joo-Young Kang https://orcid.org/0000-0002-7373-3526
Sang-Beom Seo https://orcid.org/0000-0003-4709-6022

REFERENCES

Aloia, L., Di Stefano, B., Di Croce, L. (2013). Polycomb complexes in stem cells and embryonic development. Development *140,* 2525-2534.

Aplan, P.D., Nakahara, K., Orkin, S.H., Kirsch, I.R. (1992). The SCL gene product: a positive regulator of erythroid differentiation. EMBO J. *11,* 4073-4081.

Bajaj, J., Hamilton, M., Shima, Y., Chambers, K., Spinler, K., Van Nostrand, E.L., Yee, B.A., Blue, S.M., Chen, M., Rizzeri, D., et al. (2020). An in vivo genome-wide CRISPR screen identifies the RNA-binding protein Staufen2 as a key regulator of myeloid leukemia. Nat. Cancer *1,* 410-422.

Banerjee, S., Lu, J., Cai, Q., Sun, Z., Jha, H.C., Robertson, E.S. (2014). EBNA3C augments Pim-1 mediated phosphorylation and degradation of p21 to promote B-cell proliferation. PLoS Pathog. *10,* e1004304.

Beguin, Y. (1999). Erythropoietin and platelet production. Haematologica *84,* 541-547.

Bhatlekar, S., Fields, J.Z., Boman, B.M. (2018). Role of HOX genes in stem cell differentiation and cancer. Stem Cells Int. *2018,* 3569493.

Bixby, D. and Talpaz, M. (2009). Mechanisms of resistance to tyrosine kinase inhibitors in chronic myeloid leukemia and recent therapeutic strategies to overcome resistance. Hematology Am. Soc. Hematol. Educ. Program *2009,* 461-476.

Bodenmiller, B., Campbell, D., Gerrits, B., Lam, H., Jovanovic, M., Picotti, P., Schlapbach, R., Aebersold, R. (2008). PhosphoPep--a database of protein phosphorylation sites in model organisms. Nat. Biotechnol. *26,* 1339-1340.

Bracken, A.P., Dietrich, N., Pasini, D., Hansen, K.H., Helin, K. (2006). Genome-wide mapping of Polycomb target genes unravels their roles in cell fate transitions. Genes Dev. *20,* 1123-1136.

Bruserud, O., Gjertsen, B.T., Huang, T. (2000). Induction of differentiation and apoptosis- a possible strategy in the treatment of adult acute myelogenous leukemia. Oncologist *5,* 454-462.

Daga, A., Podesta, M., Capra, M.C., Piaggio, G., Frassoni, F., Corte, G. (2000). The retroviral transduction of HOXC4 into human CD34(+) cells induces an in vitro expansion of clonogenic and early progenitors. Exp. Hematol. *28,* 569-574.

Deininger, M.W., Goldman, J.M., Melo, J.V. (2000). The molecular biology of chronic myeloid leukemia. Blood *96,* 3343-3356.

Di Carlo, V., Mocavini, I., Di Croce, L. (2019). Polycomb complexes in normal and malignant hematopoiesis. J. Cell Biol. *218,* 55-69.

Doench, J.G., Fusi, N., Sullender, M., Hegde, M., Vaimberg, E.W., Donovan, K.F., Smith, I., Tothova, Z., Wilen, C., Orchard, R., et al. (2016). Optimized sgRNA design to maximize activity and minimize off-target effects of CRISPR-Cas9. Nat. Biotechnol. *34,* 184-191.

Doyle, J.M., Gao, J., Wang, J., Yang, M., Potts, PR. (2010). MAGE-RING protein complexes comprise a family of E3 ubiquitin ligases. Mol. Cell *39,* 963-974.

Dzierzak, E. and Philipsen, S. (2013). Erythropoiesis: development and differentiation. Cold Spring Harb. Perspect. Med. *3,* a011601.

Fong, K.W., Zhao, J.C., Song, B., Zheng, B., Yu, J. (2018). TRIM28 protects TRIM24 from SPOP-mediated degradation and promotes prostate cancer progression. Nat. Commun. *9,* 5007.

Fursova, N.A., Blackledge, N.P., Nakayama, M., Ito, S., Koseki, Y., Farcas, A.M., King, H.W., Koseki, H., Klose, R.J. (2019). Synergy between variant PRC1 complexes defines polycomb-mediated gene repression. Mol. Cell *74,* 1020-1036.e8.

Hemenway, C.S., de Erkenez, A.C., Gould, G.C. (2001). The polycomb protein MPc3 interacts with AF9, an MLL fusion partner in t(9;11)(p22;q23) acute leukemias. Oncogene *20,* 3798-3805.

Jagannathan-Bogdan, M. and Zon, L.I. (2013). Hematopoiesis. Development *140,* 2463-2467.

Jiang, X. and Chen, Z.J. (2011). The role of ubiquitylation in immune defence and pathogen evasion. Nat. Rev. Immunol. *12,* 35-48.

Kim, J.Y., Kee, H.J., Choe, N.W., Kim, S.M., Eom, G.H., Baek, H.J., Kook, H., Kook, H., Seo, S.B. (2008). Multiple-myeloma-related WHSC1/MMSET isoform RE-IIBP is a histone methyltransferase with transcriptional repression activity. Mol. Cell. Biol. *28,* 2023-2034.

Klauke, K., Radulovic, V., Broekhuis, M., Weersing, E., Zwart, E., Olthof, S., Ritsema, M., Bruggeman, S., Wu, X., Helin, K., et al. (2013). Polycomb Cbx family members mediate the balance between haematopoietic stem cell self-renewal and differentiation. Nat. Cell Biol. *15,* 353-362.

Koppens, M. and van Lohuizen, M. (2016). Context-dependent actions of Polycomb repressors in cancer. Oncogene *35,* 1341-1352.

Lee, S.S., Fu, N.Y., Sukumaran, S.K., Wan, K.F., Wan, Q., Yu, V.C. (2009). TRIM39 is a MOAP-1-binding protein that stabilizes MOAP-1 through inhibition of its poly-ubiquitination process. Exp. Cell Res. *315,* 1313-1325.

Liu, Y., Shang, Y., Yan, Z., Li, H., Wang, Z., Liu, Z., Li, Z. (2019). Pim1 kinase positively regulates myoblast behaviors and skeletal muscle regeneration. Cell Death Dis. *10,* 773.

Ma, Y.N., Chen, M.T., Wu, Z.K., Zhao, H.L., Yu, H.C., Yu, J., Zhang, J.W. (2013). Emodin can induce K562 cells to erythroid differentiation and improve the expression of globin genes. Mol. Cell. Biochem. *382,* 127-136.

Mikkers, H., Nawijn, M., Allen, J., Brouwers, C., Verhoeven, E., Jonkers, J., Berns, A. (2004). Mice deficient for all PIM kinases display reduced body size and impaired responses to hematopoietic growth factors. Mol. Cell. Biol. *24,* 6104-6115.

Morey, L. and Helin, K. (2010). Polycomb group protein-mediated repression of transcription. Trends Biochem. Sci. *35,* 323-332.

Mouthon, M.A., Bernard, O., Mitjavila, M.T., Romeo, P.H., Vainchenker, W.,

Mathieu-Mahul, D. (1993). Expression of tal-1 and GATA-binding proteins during human hematopoiesis. Blood *81,* 647-655.

Oza, J., Ganguly, B., Kulkarni, A., Ginjala, V., Yao, M., Ganesan, S. (2016). A novel role of chromodomain protein CBX8 in DNA damage response. J. Biol. Chem. *291,* 22881-22893.

Park, J.W., Cho, H., Oh, H., Kim, J.Y., Seo, S.B. (2018). AURKA suppresses leukemic THP-1 cell differentiation through inhibition of the KDM6B pathway. Mol. Cells *41,* 444-453.

Park, J.W., Kang, J.Y., Hahm, J.Y., Kim, H.J., Seo, S.B. (2020). Proteosomal degradation of NSD2 by BRCA1 promotes leukemia cell differentiation. Commun. Biol. *3,* 462.

Park, S.J., Yoon, B.H., Kim, S.K., Kim, S.Y. (2019). GENT2: an updated gene expression database for normal and tumor tissues. BMC Med. Genomics *12,* 101.

Pineda, C.T., Ramanathan, S., Fon Tacer, K., Weon, J.L., Potts, M.B., Ou, Y.H., White, M.A., Potts, P.R. (2015). Degradation of AMPK by a cancer-specific ubiquitin ligase. Cell *160,* 715-728.

Saussele, S. and Silver, R.T. (2015). Management of chronic myeloid leukemia in blast crisis. Ann. Hematol. *94* Suppl 2, S159-S165.

Sawafuji, K., Miyakawa, Y., Kizaki, M., Ikeda, Y. (2003). Cyclosporin A induces erythroid differentiation of K562 cells through p38 MAPK and ERK pathways. Am. J. Hematol. *72,* 67-69.

Senthilkumar, R. and Mishra, R.K. (2009). Novel motifs distinguish multiple homologues of Polycomb in vertebrates: expansion and diversification of the epigenetic toolkit. BMC Genomics *10,* 549.

Shalem, O., Sanjana, N.E., Hartenian, E., Shi, X., Scott, D.A., Mikkelson, T., Heckl, D., Ebert, B.L., Root, D.E., Doench, J.G., et al. (2014). Genome-scale CRISPR-Cas9 knockout screening in human cells. Science *343,* 84-87.

Sutherland, J.A., Turner, A.R., Mannoni, P., McGann, L.E., Turc, J.M. (1986). Differentiation of K562 leukemia cells along erythroid, macrophage, and megakaryocyte lineages. J. Biol. Response Mod. *5,* 250-262.

Suzuki, M., Watanabe, M., Nakamaru, Y., Takagi, D., Takahashi, H., Fukuda, S., Hatakeyama, S. (2016). TRIM39 negatively regulates the NFkappaB-mediated signaling pathway through stabilization of Cactin. Cell. Mol. Life Sci. *73,* 1085-1101.

Tsiftsoglou, A.S., Vizirianakis, I.S., Strouboulis, J. (2009). Erythropoiesis: model systems, molecular regulators, and developmental programs. IUBMB Life *61,* 800-830.

van Lohuizen, M., Verbeek, S., Krimpenfort, P., Domen, J., Saris, C., Radaszkiewicz, T., Berns, A. (1989). Predisposition to lymphomagenesis in pim-1 transgenic mice: cooperation with c-myc and N-myc in murine leukemia virus-induced tumors. Cell *56,* 673-682.

Vandamme, J., Volkel, P., Rosnoblet, C., Le Faou, P., Angrand, P.O. (2011). Interaction proteomics analysis of polycomb proteins defines distinct PRC1 complexes in mammalian cells. Mol. Cell. Proteomics *10,* M110.002642.

Vu, L.P., Pickering, B.F., Cheng, Y., Zaccara, S., Nguyen, D., Minuesa, G., Chou, T., Chow, A., Saletore, Y., MacKay, M., et al. (2017). The N(6)-methyladenosine (m(6)A)-forming enzyme METTL3 controls myeloid differentiation of normal hematopoietic and leukemia cells. Nat. Med. *23,* 1369-1376.

Wang, H., Wang, L., Erdjument-Bromage, H., Vidal, M., Tempst, P., Jones, R.S., Zhang, Y. (2004). Role of histone H2A ubiquitination in Polycomb silencing. Nature *431,* 873-878.

Wang, T., Wei, J.J., Sabatini, D.M., Lander, E.S. (2014). Genetic screens in human cells using the CRISPR-Cas9 system. Science *343,* 80-84.

Wei, X., Yang, J., Adair, S.J., Ozturk, H., Kuscu, C., Lee, K.Y., Kane, W.J., O'Hara, P.E., Liu, D., Demirlenk, Y.M., et al. (2020). Targeted CRISPR screening identifies PRMT5 as synthetic lethality combinatorial target with gemcitabine in pancreatic cancer cells. Proc. Natl. Acad. Sci. U. S. A. *117,* 28068-28079.

Weng, H., Huang, H., Wu, H., Qin, X., Zhao, B.S., Dong, L., Shi, H., Skibbe, J., Shen, C., Hu, C., et al. (2018). METTL14 inhibits hematopoietic stem/progenitor differentiation and promotes leukemogenesis via mRNA m(6)A modification. Cell Stem Cell *22,* 191-205.e9.

Whichard, Z.L., Sarkar, C.A., Kimmel, M., Corey, S.J. (2010). Hematopoiesis and its disorders: a systems biology approach. Blood *115,* 2339-2347.

Zhan, X., Yang, J., Mao, Z., Yu, W. (2018). PIM1-catalyzed CBX8 phosphorylation promotes the oncogene-induced senescence of human diploid fibroblast. Biochem. Biophys. Res. Commun. *501,* 779-785.

Zhang, X. and Ren, R. (1998). Bcr-Abl efficiently induces a myeloproliferative disease and production of excess interleukin-3 and granulocyte-macrophage colony-stimulating factor in mice: a novel model for chronic myelogenous leukemia. Blood *92,* 3829-3840.

Zhou, R.Q., Gong, Y.P., Guo, Y., Shan, Q.Q., Yang, X. (2012). [The effect of knockdown of transcription factor SCL/TAL-1 gene on the erythroid differentiation in EPO-induced K562 cell line]. Zhonghua Xue Ye Xue Za Zhi *33,* 453-456. Chinese.